Supplementary Information

Enzyme immobilisation on wood-derived cellulose scaffolds *via* carbohydrate-binding module fusion constructs

A D Roberts[a†], K A P Payne[a†], S Cosgrove[a†], V Tilakaratna[a†], I Penafiel[a†], W Finnigan[a], N Turner[a†] and N S Scrutton[a†*]

[a] Manchester Institute of Biotechnology and Department of Chemistry, The University of Manchester, UK, M1 7DN

[†] EPSRC/BBSRC Future Biomanufacturing Research Hub

*Corresponding author: Professor Nigel S. Scrutton, Future Biomanufacturing Research Hub, Manchester Institute of Biotechnology and Department of Chemistry, The University of Manchester, UK, M1 7DN; E-mail: Nigel.Scrutton@manchester.ac.uk

Further experimental details

CBM-fluorescent protein construct design, expression and purification

Construct design and cloning

Genes encoding the fusion proteins were codon optimised for expression in *E. coli* using PartsGenie[1] and synthesised (Twist Bioscience). For protein expression the genes encoding the fusion protein were cloned into expression vector pBbA1c.[2] The genes of interested were amplified by PCR using CloneAmp polymerase premix (ClonTech) and the primers detailed in Table S2. The template was removed by DpnI (New England Biolabs) digest and the DNA purified using a Qiaquick PCR purification kit (Qiagen). The PCR products were cloned into NdeI/XhoI (New England Biolabs) linearised pBbA1c using Infusion HD (Clontech). DNA was transformed into NEB5alpha cells (New England Biolabs).

Protein expression and purification

An overnight preculture was grown in LB medium supplemented with 34 µg ml^{-1} chloramphenicol at 37°C. 500 ml phosphate buffered terrific broth (Formedium) supplemented with 34 µg/ml chloramphenicol at 37°C was inoculated with 5 ml pre-culture and grown at 37°C. Once the culture had reached an OD_{600} of 0.5-1 cultures were induced with 1 mM IPTG and grown at 37°C overnight. In the case of the CBM2a-mEGFP construct protein solubility was increased by dropping the incubation temperature to 25°C post-induction. The following morning cells were harvested by centrifugation and stored at -20°C until required.

Cells were resuspended in buffer A (200 mM KCl, 50 mM Tris pH 7.5) supplemented with protease inhibitor cocktail and DNAase (Sigma) and lysed by cell disruption at 20 KPsi. Lysate was clarified by ultracentrifugation at 14,000 *g* for 1 hour and the supernatant applied to a Ni-NTA agarose column (Qiagen). The column was washed with 5 column volumes of

buffer A supplemented with 10 mM imidazole and then 40 mM imidazole. The protein was eluted with buffer A supplemented with 250 mM imidazole. If required, the purified protein was concentrated in a 10k MWCO Vivaspin20 centrifugal device before being desalted into buffer A using a desalting column in order to remove the imidazole.

Protein concentration was quantified using a Cary 60 UV-vis spectrophotometer (Agilent). Extinction coefficients are detailed in Table S9. Values for A_{280} were calculated from the amino acid sequence using the Protparam tool on the ExPASy proteomics server (https://web.expasy.org/protparam/, accessed 4th March 2021) whilst extinction coefficients for the chromophores were taken from the fluorescent protein database (https://www.fpbase.org, accessed 4th March 2021).

Cellulose scaffold synthesis before DOE-based optimisation

A block of *Tilia Americana* basswood (Stockport Hobbycraft Store, UK) was sawn into 10 x 10 x 50 mm portions with the grain of the wood following the long (50 mm) axis (**Figure S1**). Each wood portion weighed approximately 0.9 – 1 g and was gently sanded by hand with abrasive paper to remove any residual wood flakes. Separately, 50 g NaOH and 25.2 g Na_2SO_3 were dissolved in DI water to a final volume of 500 ml (2.5 M NaOH, 0.4 M Na_2SO_3). 25 portions of wood were added to a 1 L round-bottomed flask before addition of the 500 ml NaOH/Na_2SO_3 solution. The mixture was then refluxed at 140 °C for 16 h with gentle magnetic stirring. The solution was then drained and the wood portions (now CSs) were washed with cold DI water 3 x times, before being refluxed with DI water (500 ml) at 125 °C for 1 hour a single time. The CSs were then refluxed in 500 ml H_2O_2 (5 %, Sigma UK) for 2 hours at 125 °C along with *ca* 5 drops of antifoam-204 (Sigma-Aldrich) (*caution: significant foaming would still occur even with antifoaming agent*). This H_2O_2 treatment was repeated two further times. The CSs were then washed in cold DI water 3 x times before being placed in 200 ml absolute ethanol overnight. DI water was then added to bring the final volume to 1 L (20 % v/v EtOH) where the CSs were then stored at room temperature (RT) until use. Informative YouTube videos of similar procedures are available online.[3,4]

CBM3A-mCherry immobilisation before DOE-based optimisation

Transparent PVC tubing (ID 8 mm, OD 12 mm) was cut to a length of approximately 80 mm. A CS would then be trimmed slightly with a razor blade into a cylindrical shape (initially cuboidal) and inserted into the tubing ensuring a tight fit and sitting in the centre of the tubing (**Figure S2a**). A 50 ml plastic Luer-Lock syringe was connected to one end of the PVC tubing using a 3-way Luer Lock valve (for loading/discharging solutions), male/female Luer Lock attachments and poly(vinylidene fluoride) (PVDF) tubing (Figure S2b). 30 ml of buffer solution (50 mM TRIS, 200 mM KCl, pH 7.5) was then flushed through the CS at a rate of 250 µL min^{-1} to flush out residual EtOH. 5 ml of CBM3A-mCherry (2 mg ml^{-1}) was then flushed through the CS at a rate of 100 µL min^{-1} (Aladin syringe pump, World Precision Instruments) and collected. A further 2 ml of buffer was flushed through and collected to wash out non-adsorbed CBM3-mCherry. The CBM3-mCherry concentration before (*ca* 2 mg ml^{-1}) and after passing though the CS (including 2 ml additional flush) was measured *via* UV-visible spectrophotometry (Abs [587], Ɛ = 72000 M^{-1} cm^{-1}, M_w = 48892.28 g mol^{-1}). The experiments were conducted at room temperature (RT, typically 19 ±3 °C).

Details of the initial CS immobilisation scoping trials

Methyl-red, a water-soluble pH sensitive dye, was employed for these trials due to availability and for its intense colouration allowing facile concentration determination by UV-Vis spectrophotometry. The pH sensitivity would also roughly indicate the pH of the CSs (red at pH 4.4 and below, yellow at pH 6.2 and above) and therefore if any residual NaOH remained from the Kraft process. The trial experiments revealed the adsorption of a saturated solution of Methyl-red (20 ml vol., flow rate 1 ml min¬-1) to the CSs and a pH-induced colour change from yellow to red – indicating an acidic nature of the CSs (likely from carboxylic acid groups). The dye appeared to have stronger adsorption at the end of the CS where the dye entered than the end where the dye exited, forming a gradient (see image below).

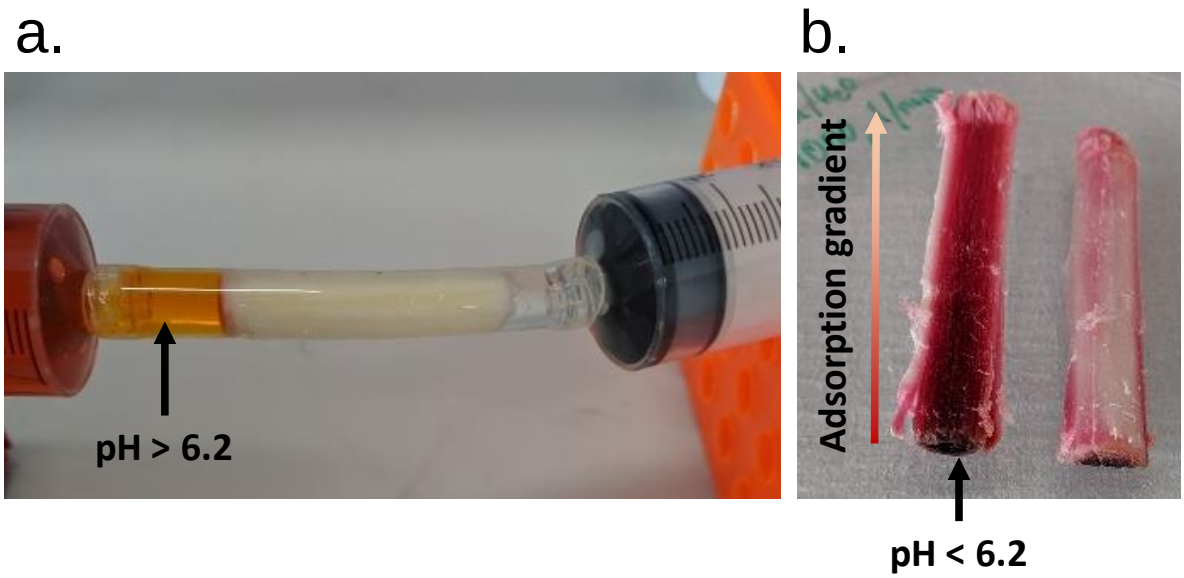

a) Basic flow set-up with Me-Red in DI water before flowing through. b) Cross-section of CS after flowing through Me-Red solution

After establishing a working procedure with Methyl-red, small quantities of the recombinant CBM-FP proteins produced and purified from the expression trials were flowed through the CSs, with concentration being measured before and after to determine immobilisation efficiency and total protein loading (see image below). The volume of each CMB-FP was made up to 5 ml, but differed in concentration due to variability in expression yield (Table S4). The results revealed successful immobilisation of each CBM-FP construct, with some having concentrations too low for detection after flushing through (implying close to 100 % immobilisation efficiency), and after an additional 1.5 ml of buffer to flush out any non-adsorbed protein. The variability in initial concentration made comparisons between CBM-FPs difficult, but CBM3A-mCherry was selected for use in the optimisation trials due to its relatively high expression yield in comparison to the other CBM-FP constructs, and its relatively high total loading (0.4 wt. %) and immobilisation efficiency (59.8 %) determined from this trial.

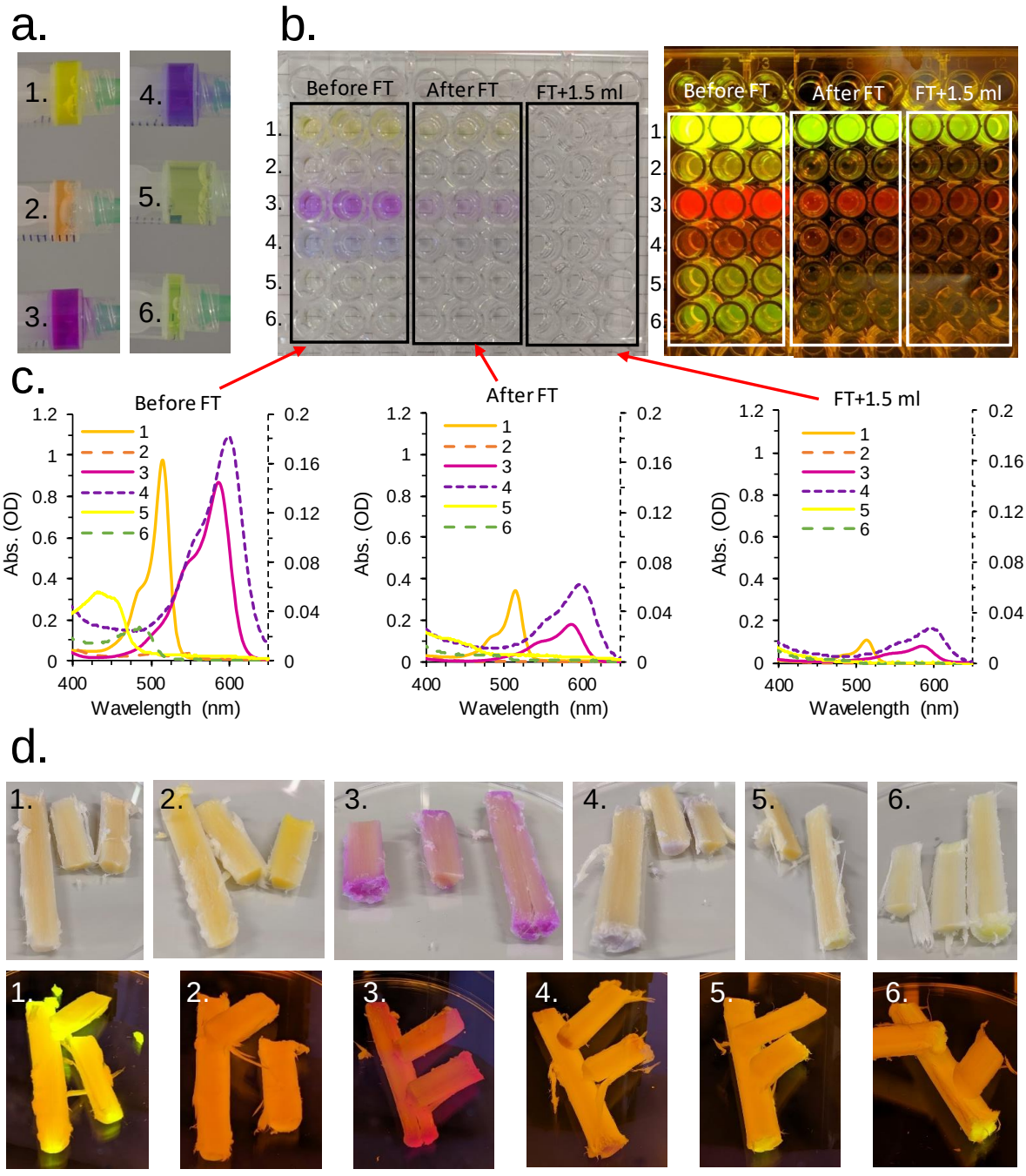

a) CBM-FP proteins purified from expression trials (prior to dilution to 5 ml): 1. mCitrine-CBM1, 2. CBM30-mOrange, 3. CBM3A-mCherry, 4. mNeptune-CBM28, 5. mECFP-CBM2A and 6. CBM2a-mEGFP. b) 96-well plate of the CBM-FP solutions before and after CS flowing through (FT), and after a subsequent 1.5 ml FT of buffer, under ordinary light (left) and a black light (right). c) UV-vis spectrophotometry traces of the CBM-FPs before (left) and after (centre) FT, and after a further 1.5 ml FT of buffer (right). d) Visible light (above) and black light (below) images of the cut-up CS's after FT and 1.5 ml buffer flush.

Details of the Bradford-chromophore protein concentration normalisation factor calculations

The calculated concentration of CBM2a-mEGFP differed significantly when measured using via the Bradford method or via its chromophore absorbance. Since the CBM2a-ωTA construct could only be measured via the Bradford method (since it has no chromophore), a normalisation factor was employed to allow direct comparison between CBM2a-ωTA and the other CBM-FP constructs (see section 3.6.1 for details).

The normalisation factor (NF) was calculated using the following equation:

$$NF = \frac{[FP]_{Abs\ 488}}{[FP]_{Bradford}}$$

Where $[FP]_{Abs\ 488}$ and $[FP]_{Bradford}$ are the calculated CBM2a-mEGFP concentrations via absorbance at 488 nm and via the Bradford method, respectively. The normalised concentration of CBM2a-ωTA construct ($[\omega TA]_{norm}$) was then calculated using the following equation:

$$[\omega TA]_{norm} = [\omega TA]_{Bradford} * NF$$

Where $[\omega TA]_{Bradford}$ is the concentration of the CBM2a-ωTA construct determined by the Bradford method. The value of the normalisation factor was calculated to be 2.93.

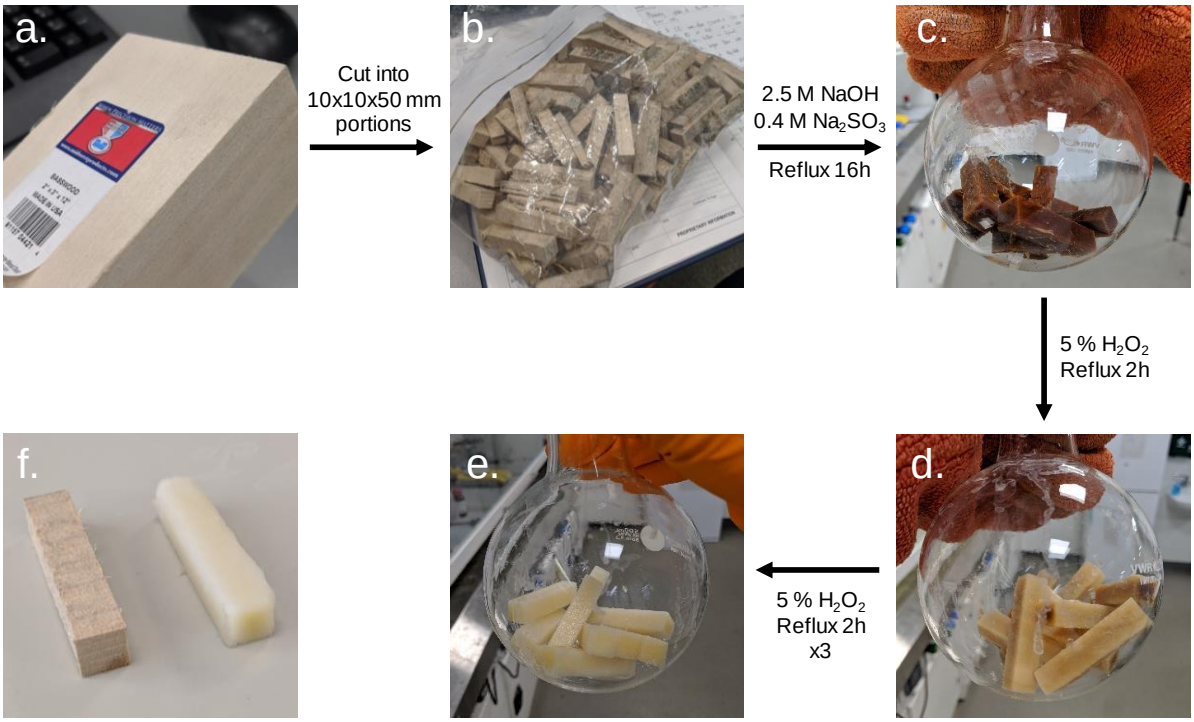

Figure S1. a) – e) Schematic depicting the initial CS synthesis protocol. f) Basswood portion (left) and processed CS (right) for comparison

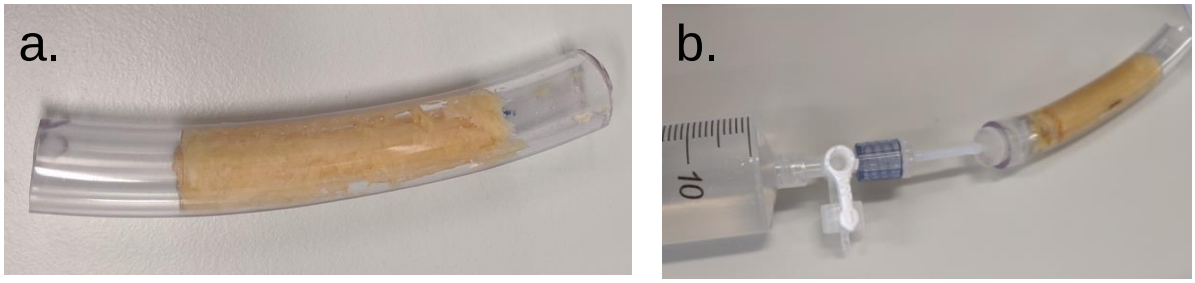

Figure S2. a) A representative CS inserted into 80 mm length PVC tubing. b) Image of syringe-tubing connection via Luer-lock attachments

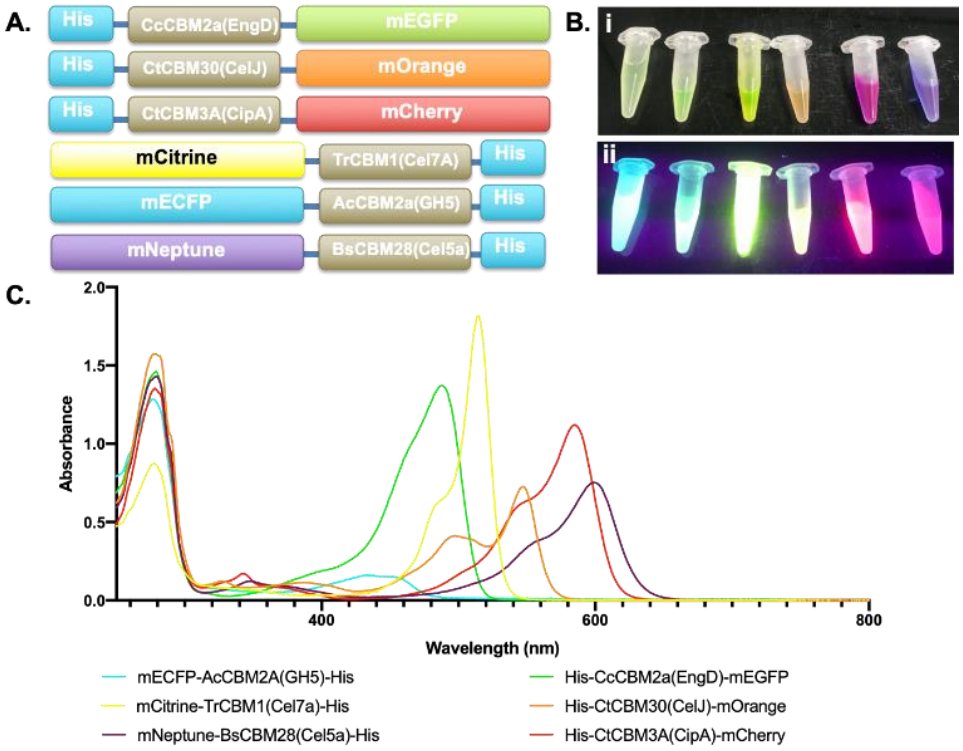

Figure S3. Characterisation of CBM-Reporter Constructs: a) Schematic of the six CBM-reporter constructs. b) Purified proteins under (i) white light and (ii) UV (from left to right, mECFP-CBM2A, CBM2a-mEGFP, mCitrine-CBM1, CBM30-mOrange, CBM3A-mCherry and mNeptune-CBM28. c) UV-vis spectra of the purified proteins.

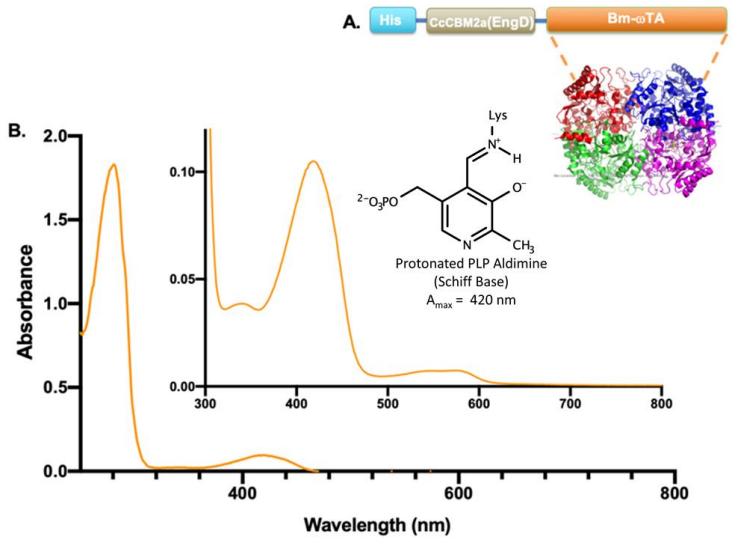

Figure S4. Characterisation of CBM2a-ωTA fusion construct. a) Schematic of the CBM-ωTA construct. b) UV-vis spectra of the purified protein. Inset, close up of the spectral features in 300 – 800 nm region resulting from the PLP cofactor.

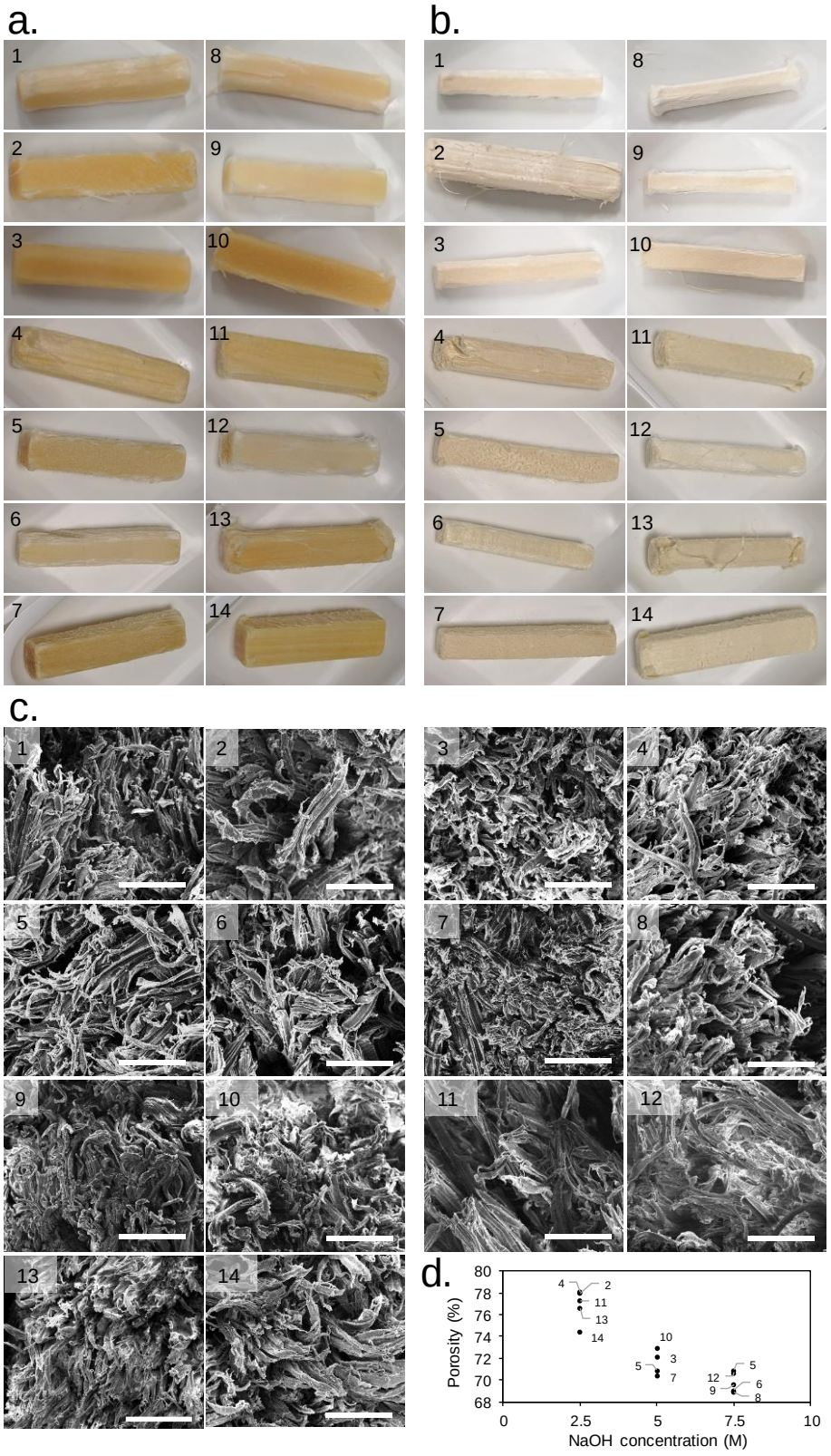

Figure S5. Numbers 1 – 14 represent the CS synthesis conditions given in Table 2. a) Visible light images of CSs soaked in acetone and b) after drying. c) FEG-SEM images of the end of each CS showing loss of ordered structure (fibrillation). Scale bar = 100 µm d) Plot showing variation of CS porosity with increasing NaOH concentration during Kraft process

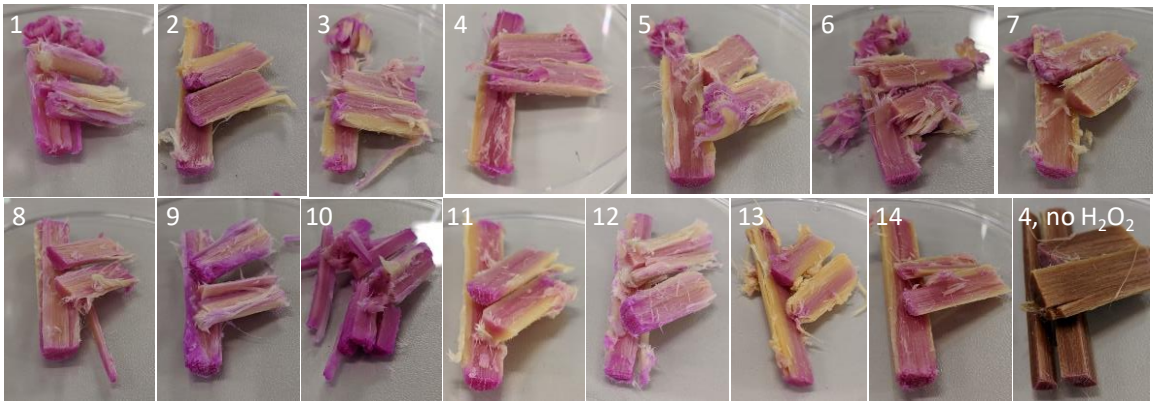

Figure S6. Visible light images of CS's produced under the synthesis conditions given in Table 2 after flowing-through CBM3-mCherry solution and cutting up

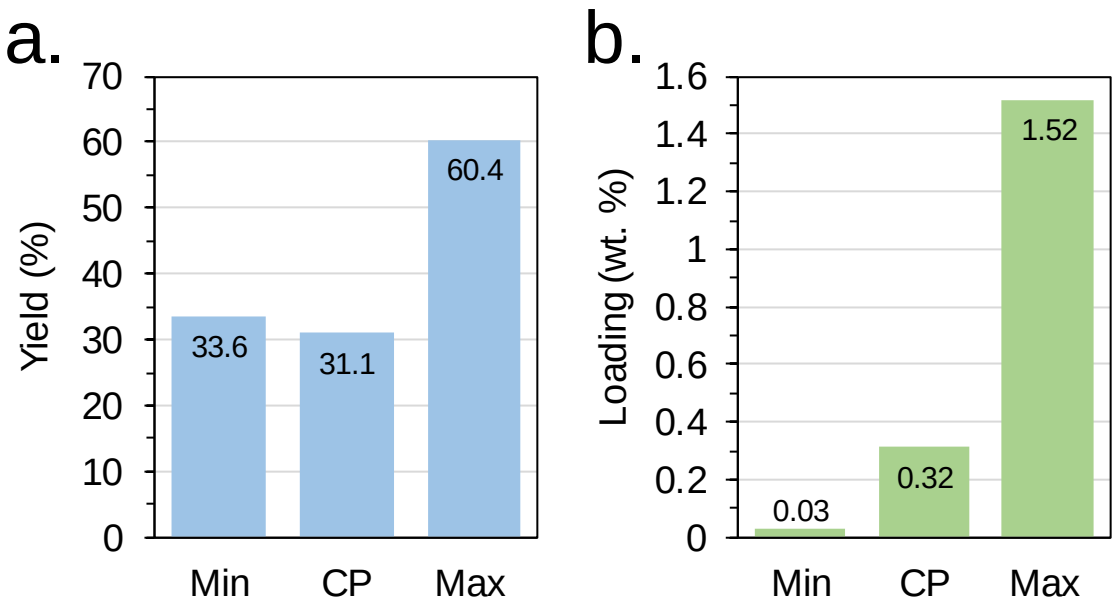

Figure S7. a) Immobilisation yield and b) loading results for the flow conditions scoping trials showing minimum (Min) and maximum (Max) forcing and centre-point (CP) conditions

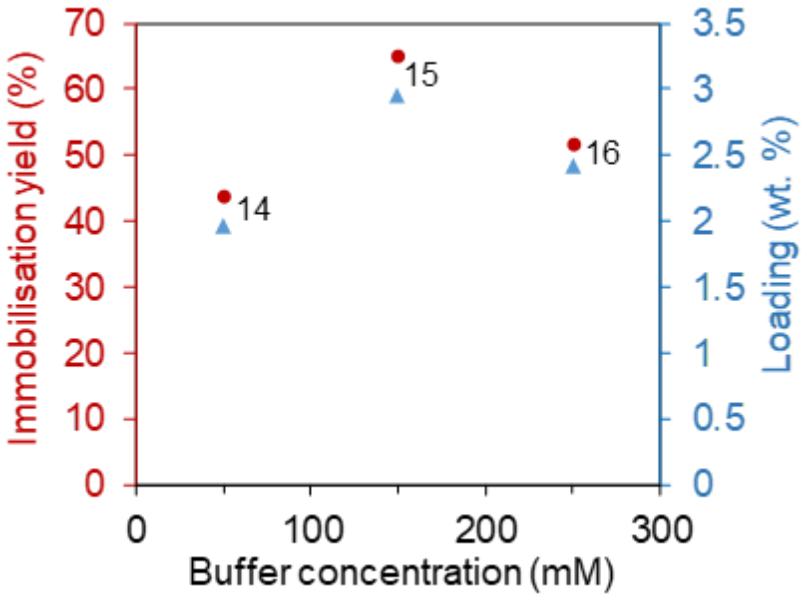

Figure S8. Experiments 14, 15 and 16 of the flow conditions optimisation DOE: immobilisation yield (red dots) and loading (blue triangles) with increasing buffer concentration

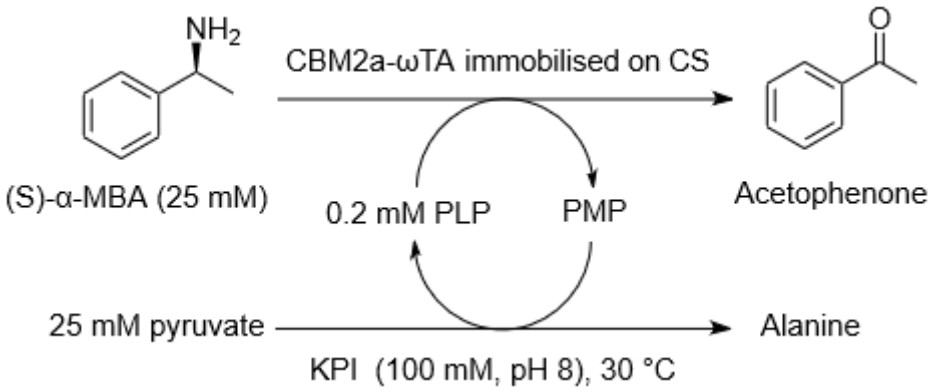

Figure S9. Reaction scheme depicting the conversion of (S)-α-MBA into acetophenone via the CS immobilised CBM2a-ωTA enzyme

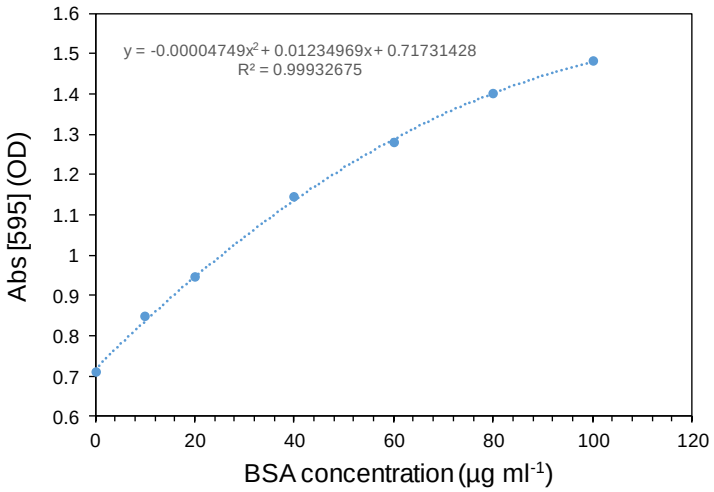

Figure S10. Bradford assay calibration curve employing BSA as a standard

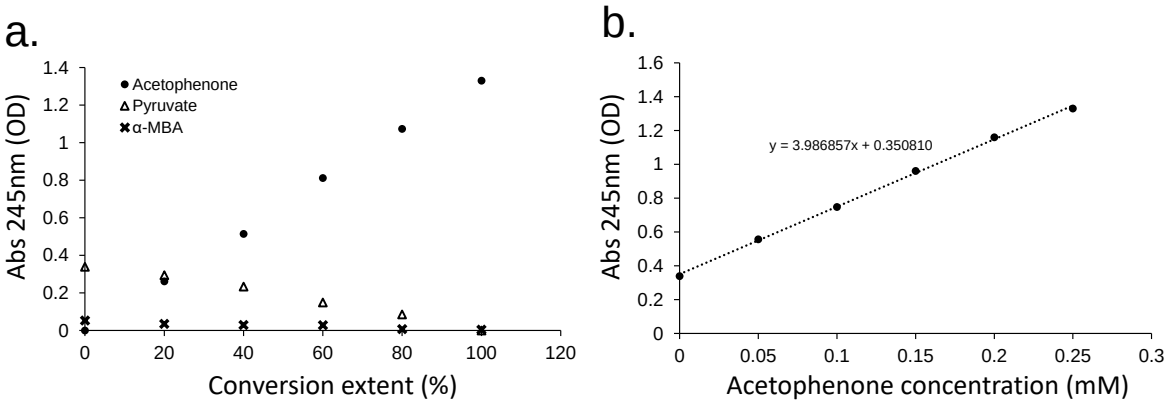

Figure S11. a) Individual calibration curves for acetophenone, pyruvate and α-MBA at 245 nm based on theoretical conversion extent. b) Summed calibration curves allowing monitoring of acetophenone production.

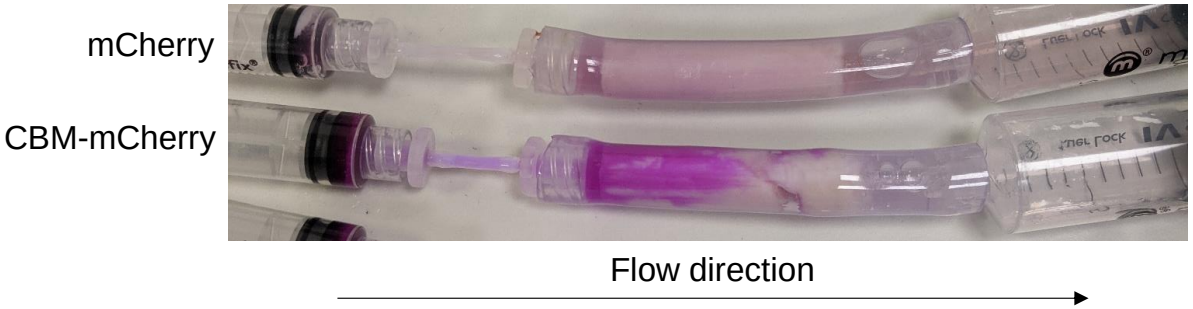

Figure S12. Visible light images of the CS's after having cell lysate containing mCherry (above) and CBM3a-mCherry (below) flowed through.

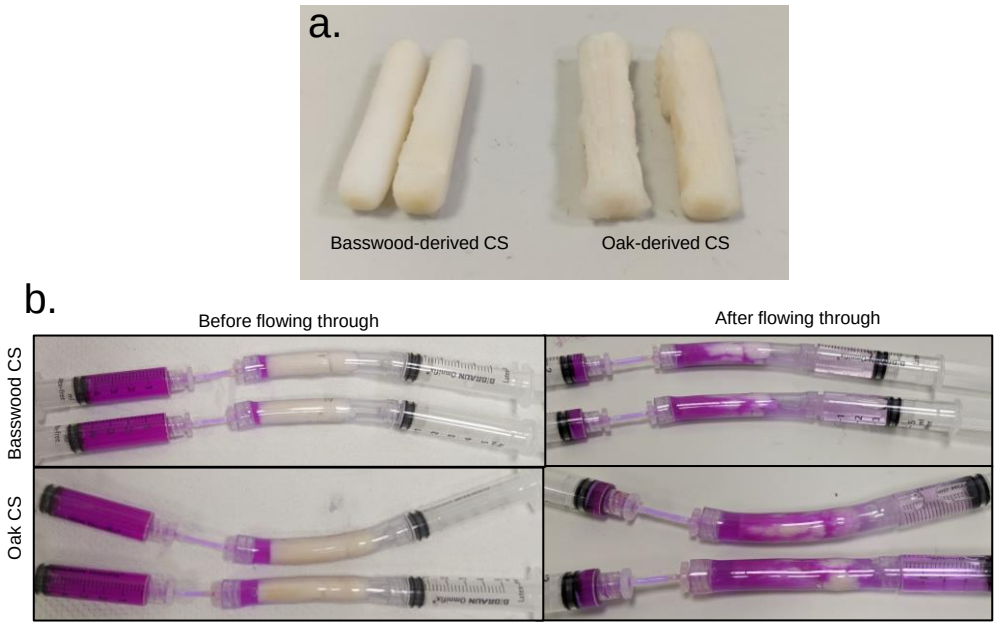

Figure S13. Camera images of Basswood (left) and Oak (right) derived CSs. b) camera images of the above before (left) and after (right) flowing through CBM3a-mCherry.

Table S1. Summary of previously reported enzyme immobilisation techniques employing CBM-based affinity binding in comparison with results from this study. NR = Not reported. Numbers in parentheses denote values after a 10 ml buffer flush.

Cellulose support	Protein/Enzyme	CBM	Loading (wt. %)	Immobilisation efficiency (%)	Ref
Microcrystalline cellulose (Avicel®)	*Cis*-epoxysuccinic acid hydrolase (CESH) from *Rhodococcus opacus*	CcCBM2a from *Clostridium cellulovorans* (EngD)	1.97 ±0.12	NR	5
		CcCBM3 from *Clostridium* cellulolyticum (CipC)	2.00 ±0.05		
		CtCBM3 from *Clostridium thermocellum* (CipA)	1.22 ±0.26		
		CtCBM11 from *C. thermocellum* (CelH)	1.26 ±0.07		
		CtCBM30 from *C. thermocellum* (CelJ)	0.79 ±0.06		
Microcrystalline cellulose (Avicel®)	Lipase from *Bacillus stearothermophilus*	ThCBM from *Trichoderma hazianum*	0.112 ±0.04	NR	6
Bacterial microcrystalline cellulose	Lipase B from *Candida antarctica*	NpCBM from *Neocallimastix patriciarum* (Cel6A)	NR	NR	7
Microcrystalline cellulose (unspecified source)	Glucoamylase from *Neurospora crassa*	NcCBM from *N. crassa* (Cbh-1)	NR	NR	8
Microcrystalline cellulose (Sigmacell® Type 20)	Atrazine chlorohydrolase	CtCBM from *C. thermocellum*	NR	NR	9
		CcCBM from *C. cellulovorans*			
Microcrystalline cellulose (Sigmacell® Type 20)	Horseradish peroxidase from *Armoracia rusticana*	CcCBM from *C. cellulovorans* (CbpA)	2.2	NR	10
Microcrystalline cellulose (Avicel®)	Organophosphate hydrolase from *Flavobacterium*	CcCBM from *C. cellulovorans* (CbpA)	NR	NR	11
Microcrystalline cellulose (Avicel®)	Lipase B from *Candida antarctica*	NpCBM from *N. patriciarum* (CelA)	NR	NR	12
Bacterial cellulose membrane	*β*-galactosidase from *T. maritima*	PfCBM2 from *P. furiosus* chitinase	1.85	81 ±4	13
Insoluble β-1,3-glucan (Curdlan)	Chitosanase from *Gynuella sunshinyii*	CBM56 (β-1,3-glucan-binding domain) from *Paenibacillus barengoltzii*	NR	90.1	14
Cellulose nanogel from microcrystalline cellulose	Lipase from *Geobacillus stearothermophilus*	CBM (unspecified)	NR	~92	15
Microcrystalline cellulose (Avicel® and Sigmacell®)	Lipase S-2 from *Cryptococcus sp.*	CBM from *T. reesei* (Cbh-1)	NR	~85 – 90	16
Microcrystalline cellulose powder, 25 µm (Aladdin Chemistry®)	β-glucosidase Bgl1A(A24S/F297Y)	CBM3 from Tramates sp. AH28-2	NR	NR	17
		CBM24 from C. thermocellum (HF912724.1			
		CBM60 from C. cellulovorans (743B)			

		CBM67 from Ruminiclostridium thermocellum (CCV01467.1)			
		CBM91 from Cellulosilyticum ruminicola (JCM 14822)			
		CBM92 from R. thermocellum, (AAA20892.1)			
Wood-derived aligned CSs: *conditions for high loading*	mEGFP	CcCBM2a from *C. cellulovorans* (EngD)	4.59 (3.94)	91.8 (78.7)	This work
	mCherry	CtCBM3A from *C. thermocellum* (CipA)	5.24 (4.63)	79.4 (70.1)	
	mOrange	CtCBM30 from *C. thermocellum* (CelJ)	3.22 (1.88)	51.8 (30.2)	
	mCitrine	TrCBM1 from *Trichoderma reesei* (Cel17A)	NR	NR	
	mECFP	AcCBM2A from *Acidothermus cellulolyticus* (GH5)	NR	NR	
	mEGFP *[control]*	None	3.43 (1.05)	78.1 (24.0)	
	mCherry *[control]*	None	2.02 (0.34)	40.9 (6.9)	
	ωTA from *B. megaterium*	CcCBM2a from *C. cellulovorans* (EngD)	3.99± 0.86	62.1 ±8.9	
Wood-derived aligned CSs: *conditions for high immobilisation efficiency*	mEGFP	CcCBM2a from *C. cellulovorans* (EngD)	2.88 (2.38)	97.1 (80.2)	This work
	mNeptune	BsCBM28 from *Bacillus sp. 1139* (Cel5a)	2.11 (1.60)	69.5 (52.9)	
	ωTA from *B. megaterium*	CcCBM2a from *C. cellulovorans* (EngD)	2.34 (1.72)	81.4 (60.3)	
Wood-derived **non-aligned** cellulose scaffolds [control]: *conditions for high loading*	mCherry	CtCBM3A from *C. thermocellum* (CipA)	5.91 (4.15)	91.3 (64.1)	This work

Table S2. List of the primers employed in this study

Name	Sequence
pBbA1cvCATHisFw	AAGGAGATATACATATGgcacaccaccacc
pBbA1cmNeptuneFw	AAGGAGATATACATATGgtttctaaaggagaagaactg
pBbA1cmECFPFw	AAGGAGATATACATATGgttagcaaaggagaggaac
pBbA1cmCitrineFw	AAGGAGATATACATATGgtatcgaaaggtgaggaattg
pBbA1cXhoIsuffixRv	GAGATCCTTACTCGAGtttggatccgagtc
CcCBM2aEngDBMwTAF	GGCAGTGGAGAGCTCATGAGCCTGACCGTGCAG
HindIIISuffixBmwTAR2	AGTCTACAAAAGCTTTTATGCCTGCCATTCACCG
HindIIISuffixF	AAGCTTTTGTAGACTCGGATCCA
HisCcCBM2aEngDR	GAGCTCTCCACTGCCGCT

Table S3. Summary of the design of the CBM-FP constructs

Name	N-term	Linker	C-term
CBM2a-mEGFP	His-CcCBM2a(EngD)	GSSAGSSAAGSGSG	mEGFP
CBM30-mOrange	His-CtCBM30(CelJ)	GSSAGSSAAGSGSG	mOrange
CBM3A-mCherry	His-CtCBM3A(CipA)	RGTTTTRRPATTTGSSPGPTQS	mCherry
mCitrine-CBM1	mCitrine	RGTTTTRRPATTTGSSPGPTQS	TrCBM1(Cel17A)-His
mECFP-CBM2A	mECFP	RGTTTTRRPATTTGSSPGPTQS	AcCBM2A(GH5)-His
mNeptune-CBM28	mNeptune	RGTTTTRRPATTTGSSPGPTQS	BsCBM28(Cel5a)-His

Table S4. Summary of initial scoping trials probing CBM-FP immobilisation to CS's

	Protein	**Expression yield (mg L^{-1})**	**Initial concentration (µg ml^{-1})**	**Amount immobilised (µg)**	**Immobilisation yield (%)**	**Loading (wt. %)**
1	mCitrine-CBM1	3.67	733.8	935.0	31.9	0.148
2	CBM2-mOrange	0.20	40.20	160.8	100	0.0267
3	CBM3-mCherry	5.1	1020	2443	59.8	0.400
4	mNeptune-CBM4	1.34	268.4	333.6	31.1	0.0543
5	CFP-CBM5	0.61	121.0	483.9	100	0.0765
6	CBM6-GFP	0.17	33.60	134.4	100	0.0226

Table S5. Summary of main factors involved in the CS synthesis DSD

Factor	Categorisation	Inclusion in DSD? (Y/N)	Value and range	Units
NaOH conc.	Numerical	Y	2.5 – 7.5	M
Na_2SO_3 conc.	Numerical	Y	0.4 – 1.2	M
Sulphite processing vol.	Numerical	Y	100 - 250	ml
H_2O_2 conc.	Numerical	Y	4 - 12	vol. %
H_2O_2 vol.	Numerical	Y	100 – 250	ml
Mass of wood portions	Numerical	N	4.5 – 5	g
Flask size	Categorical	N	1000	ml
Sulphite processing duration	Numerical	N	16 – 18	h
No. of water washes (RT)	Categorical	N	3	n
No. of water washes (reflux)	Categorical	N	3	n
No. of H_2O_2 treatments (reflux)	Categorical	N	1	n
Protein type	Categorical	N	CBM3-mCherry	n/a
Immobilisation conditions	mix	N	Initial immobilisation procedure	n/a
CS storage conditions	mix	N	20% EtOH	n/a

Table S6. Summary of output variables and other characteristics of the CS's produced from the CS synthesis DSD

Experiment No.	Protein loading (wt. %)	Immobilisation yield (%)	Porosity (%)	I_{max}/I_{110}	Cellulose polymorph	Shrinkage on drying
1	0.71	42.3	70.9	2.88	II	High
2	0.52	29.5	78.0	5.43	Iβ	Low
3	0.64	39.7	72.1	3.57	Iβ	High
4	0.69	47.1	78.1	3.85	Iβ	Low
5	0.35	28.8	70.9	3.73	Iβ	Medium
6	0.54	41.7	69.1	3.75	II	High
7	0.60	34.5	70.4	5.79	Iβ	Low
8	0.81	52.4	68.9	3.77	II	High
9	0.59	42.6	69.6	5.03	II	High
10	0.52	39.2	73.0	5.22	Iβ	Medium
11	0.25	15.9	77.3	4.13	Iβ	Low
12	0.26	18.4	70.7	3.64	II	High
13	0.28	17.5	76.6	3.79	Iβ	Medium
14	0.18	11.8	74.5	3.43	Iβ	Low
15	0.83	49.4	-	3.55	Iβ	-
16	1.01	59.5	-	-	-	-
17	1.15	67.1	-	-	-	-
18	1.09	70.5	-	-	-	-
PB	-	-	72.3	-	-	-
4 no H_2O_2	-	-	72.6	6.14	Iβ	Low

Table S7. Summary of main factors involved in the flow conditions optimisation DSD

Factor	Categorisation	Inclusion in DSD? (Y/N)	Value and range	Units
Protein conc.	Numerical	Y	0.5 – 5	mg ml^{-1}
Protein vol.	Numerical	Y	2.5 – 7.5	Ml
pH	Numerical	Y	7.1 – 9.1	n/a
Flow rate	Numerical	Y	50 – 250	µl min^{-1}
Salt conc.	Numerical	Y	10 – 300	mM
Buffer conc.	Numerical	N	50	mM
Salt type	Categorical	N	KCl	n/a
Buffer type	Categorical	N	TRIS	n/a
Protein type	Categorical	N	CBM3-mCherry	n/a
Buffer type	Categorical	N		
CS synthesis conditions	Mix	N	Initial CS synthesis conditions	n/a
Temperature	Nuisance	N	19 ±2	°C

Table S8. Summary of the CS immobilisation data for the CBM2a-ωTA and CBM2a-mEGFP constructs

Construct	Quantification method	Initial protein concentration (mg ml^{-1})	Initial loading (wt. %)	Loading after 10 ml flush (wt. %)	Initial immobilisation efficiency (%)	Immobilisation efficiency after 10 ml flush (%)
CBM2a-ωTA	Bradford assay	2.25	0.80	0.59	81.4	60.3
CBM2a-mEGFP	Bradford assay	1.7	0.71	0.53	95.5	71.6
	Abs 488 nm	4.98	1.94	1.30	94.2	68.7
CBM2a-ωTA	[Normalised]	6.68	2.34	1.72	81.4	60.3

Table S9. UV-vis parameters used for protein quantification

Construct	**Ext. Coeff. 280nm ($cm^{-1}M^{-1}$)**	**Chromophore**	**Wavelength (nm)**	**Ext. Coeff. Chromophore ($cm^{-1}M^{-1}$)**
mNeptune-CBM28	70820	mNeptune	600	60,000
CBM30-mOrange	79300	mOrange	548	71,000
mECFP-CBM2A	52370	mECFP	433	32,500
mCitrine-CBM1	29340	mCitrine	516	77,000
CBM3A-mCherry	69790	mCherry	587	72,000
CBM2a-mEGFP	48360	mEGFP	488	56,000

References

1 N. Swainston, M. Dunstan, A. J. Jervis, C. J. Robinson, P. Carbonell, A. R. Williams, J.-L. Faulon, N. S. Scrutton and D. B. Kell, *Bioinformatics*, 2018, **34**, 2327–2329.

2 T. S. Lee, R. A. Krupa, F. Zhang, M. Hajimorad, W. J. Holtz, N. Prasad, S. K. Lee and J. D. Keasling, *J. Biol. Eng.*, 2011, **5**, 12.

3 AvE, Making WOOD GLASS | Home Chemistry Experiment, https://www.youtube.com/watch?v=880a_XgvBEo, (accessed 25 March 2020).

4 NileRed, Making transparent wood, https://www.youtube.com/watch?v=x1H-323d838, (accessed 25 March 2020).

5 S. Wang, G.-Z. Cui, X.-F. Song, Y. Feng and Q. Cui, *Appl. Biochem. Biotechnol.*, 2012, **168**, 708–717.

6 S. Hwang, J. Ahn, S. Lee, T. G. Lee, S. Haam, K. Lee, I.-S. Ahn and J.-K. Jung, *Biotechnol. Lett.*, 2004, **26**, 603–605.

7 M. Gustavsson, J. Lehtiö, S. Denman, T. T. Teeri, K. Hult and M. Martinelle, *Protein*

Eng., 2001, **14**, 711–715.

8 M. Jiang and A. Radford, *Enzyme Microb. Technol.*, 2000, **27**, 434–442.

9 C. Kauffmann, O. Shoseyov, E. Shpigel, E. A. Bayer, R. Lamed, Y. Shoham and R. T. Mandelbaum, *Environ. Sci. Technol.*, 2000, **34**, 1292–1296.

10 I. Levy, G. Ward, Y. Hadar, O. Shoseyov and C. G. Dosoretz, *Biotechnol. Bioeng.*, 2003, **82**, 223–231.

11 R. D. Richins, A. Mulchandani and W. Chen, *Biotechnol. Bioeng.*, 2000, **69**, 591–596.

12 J. C. Rotticci-Mulder, M. Gustavsson, M. Holmquist, K. Hult and M. Martinelle, *Protein Expr. Purif.*, 2001, **21**, 386–392.

13 B. N. Estevinho, N. Samaniego, D. Talens-Perales, M. J. Fabra, A. López-Rubio, J. Polaina and J. Marín-Navarro, *Int. J. Biol. Macromol.*, 2018, **115**, 476–482.

14 S. Lin, Z. Qin, Q. Chen, L. Fan, J. Zhou and L. Zhao, *J. Agric. Food Chem.*, 2019, **67**, 6847–6855.

15 A. Kumar, S. Zhang, G. Wu, C. C. Wu, J. Chen, R. Baskaran and Z. Liu, *Colloids Surfaces B Biointerfaces*, 2015, **136**, 1042–1050.

16 J. Thongekkaew, H. Ikeda and H. Iefuji, *Biochem. Biophys. Res. Commun.*, 2012, **420**, 183–187.

17 F. Chang, S. Xue, X. Xie, W. Fang, Z. Fang and Y. Xiao, *J. Biosci. Bioeng.*, 2018, **125**, 185–191.